

Compression Isotherms of Argon, Krypton, and Xenon Through the Freezing Zone

P. H. LAHR and W. G. EVERSOLE

Linde Co., Division of Union Carbide Corp., Tonawanda, N. Y.

THE FREEZING point of argon as a function of pressure was determined experimentally by Simon, Ruhemann, and Edwards (6) at pressures up to 5000 atm., by Bridgman (2) up to 5800 atm., and by Robinson (5) up to 9000 atm. The freezing point at 12,600 atm. and 20° C. was determined by Robertson (1). Bridgman (2) also measured the change in volume of argon during freezing below 5800 atm. Apparently no measurements of this type have previously been reported for krypton or xenon.

New data are presented here for argon and the work has been extended to include krypton and xenon. The freezing pressures of argon, krypton, and xenon, the changes in volume during freezing, and approximate compressibilities of the solid and gas near the freezing point in the temperature range 140° to 360° K. have been determined. In the case of xenon, the compressibility of the solid was measured up to 22,000 atm., which is well beyond the freezing pressure. The volume change of argon during freezing was found to be larger and to decrease more slowly with increasing pressure than reported by Bridgman (2).

In this work, the temperatures, pressures, and volumes were measured during both freezing and melting. Single-line isotherms were then constructed from these data by averaging the hysteresis. It is assumed that the conditions for freezing and melting are identical and that the terms "melting point" and "freezing point" are interchangeable.

APPARATUS AND PROCEDURE

Figure 1 shows the essential parts of the apparatus. The core of the pressure vessel was very nearly cylindrical; it was 4 inches high, 0.5 inch in I.D., and 3 inches in O.D. It was made of Bearcat tool steel (Rockwell C-55) press-fitted with 15-mils interference on the 3-inch diameter into a larger cylinder of R_c-45 alloy steel 3-¼ inches high and 6 inches in O.D. A gas lead of ¼₁₆-inch stainless steel tubing, secured to the protruding portion of the inner cylinder by a Midget high-pressure fitting, emerged flush with the inner surface of the vessel at a point 0.95 inch from the top. Bridgman-type seals having a nominal 14% unsupported area were used with Teflon gaskets and Bearcat steel R_c-55 buttons to close the vessel. A thermocouple was inserted in the lower seal in a hole drilled to within ⅛ inch of the gas space. A jacket around the assembly permitted the circulation of hot or cold fluid to maintain the desired temperature. The assembly was mounted between the platens of a 70-ton press.

Pressure and press movement were recorded on an x-y recorder (Houston Instrument Co.). Pressure was measured by a load cell mounted directly above the upper piston. The load cell consisted of a strain gage bridge containing two Baldwin AB-20, 1000-ohm gages mounted vertically on flats on a hardened steel piston, and two unloaded dummy gages. The load cell was calibrated against a 12-inch Heise gage in the oil line to the press. The cell was checked against the freezing pressure of water and the center of the hysteresis loop for ice VI was found to correspond to Bridgman's value.

The press movement was measured by a Bourne's linear potentiometer mounted solidly to the fixed upper platen of the press. Piston travel was taken as the difference

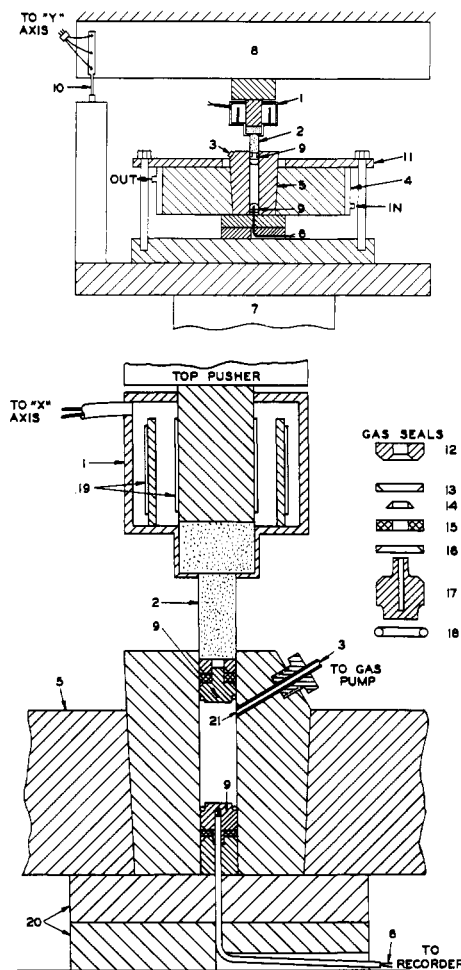


Figure 1. Essential parts of the apparatus used (top) and enlarged view of chamber (bottom)

- | | |
|----------------------------|----------------------|
| 1. Load cell | 11. Flange |
| 2. Tungsten carbide piston | 12. Pusher |
| 3. Gas inlet | 13. Steel ring |
| 4. Cooling jacket | 14. Steel inner ring |
| 5. Vessel | 15. Teflon spacer |
| 6. Thermocouple lead | 16. Brass ring |
| 7. Moving platen | 17. Button |
| 8. Stationary platen | 18. O ring |
| 9. Gas seals | 19. Strain gages |
| 10. Linear extensometer | 20. Base plates |

between the press movement and extraneous compression of the piston, gaskets, and supporting members of the vessel. The volume of the interior of the vessel and the true height of the piston (as distinguished from the extraneous compression as a function of load) were determined by a check run with water in the vessel, using Bridgman's values for the compressibility of water. The correction for extraneous compressibility was refined by a run with just sufficient glycerol in the vessel to separate the pistons, using Bridgman's values for the compressibility of glycerol.

To begin a run with argon, the line and vessel were purged and the gas was compressed into the vessel at room temperature and at about 1000 atm. The upper piston (Figure 1) was advanced (by bleeding oil to the press)

to seal off the inlet port in the vessel; then the piston was further advanced very slowly to reach the desired pressure. Two to 4 hours were required to reach 18,000 atm., the rate of compression being especially low during freezing of the argon in order that the heat of fusion would be dissipated with less than 1° C. rise in temperature. Isothermal expansion of the argon back through the melting zone required another 2 to 4 hours.

Krypton and xenon were handled similarly, except that the vessel was cooled below room temperature before it was filled, and the gas was charged into the vessel at a much lower pressure. The vessel was then brought to room temperature to improve the seal and the upper piston was advanced to close the inlet port. Once the gaskets formed a seal at room temperature, they could be depended upon to hold at lower temperatures.

Linde cylinders of argon, krypton, and xenon were used in this work. Each of the gases exceeded 99.99% in purity. Since argon was at all times well above atmospheric pressure, no air leaks into the system were possible. Freedom from contamination of krypton and xenon is less certain. However, an attempt was made to keep the charging line at a positive pressure.

At the end of each series of tests, the gas was removed and its quantity measured. In the case of argon, the measurements thus made were checked in the lower end of the pressure range (where published data on the density were available) by calculating how much argon was present in the pressure vessel, using figures for the measured volume, pressure, and temperature and the literature values for the density. The calculated argon quantities checked the measured quantities very well. Gas could be kept in

the vessel for several weeks with no apparent loss. Quantities of krypton and xenon as determined by the volume of the vessel and published *PVT* data were always slightly higher than the amount subsequently recovered due in part to gas adsorbed in the *o* ring. Consequently, calculated quantities were considered to be the more reliable.

Figure 2 shows typical *x-y* curves of raw data. The lower line is the correction curve for extraneous press motion. The two upper lines show press motion *vs.* oil pressure to the press during compression and expansion of argon at constant temperature. An idealized curve is drawn midway between the two upper curves, and the change in volume during freezing is obtained from the vertical height between the fluid and solid portions of the idealized curve.

RESULTS FOR ARGON

Argon was compressed isothermally through its freezing pressure at temperatures ranging from 137° to 368° K. and at pressures up to 18,000 atm. The raw data are given in Table I.

The effect of pressure on the melting point of argon is shown graphically in Figure 3, together with the data of Bridgman (2) and the single value obtained by Robertson (1). The solid line is a graph of the Simon (6) melting equation:

$$P_m/P_0 = (T_m/T_0)^c - 1$$

where P_m and T_m are the melting pressure and temperature, P_0 is the internal pressure, T_0 is the melting temperature extrapolated to zero pressure, and c is a constant. The value used for T_0 was 83.2° K., from Bridgman (2). The

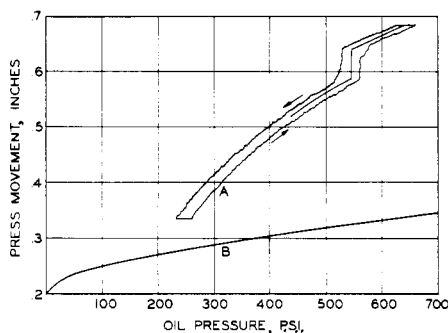


Figure 2. Experimental *x-y* curve

- A. Press movement vs. oil pressure for compression of argon at 15° C.
B. Correction curve for extraneous press motion

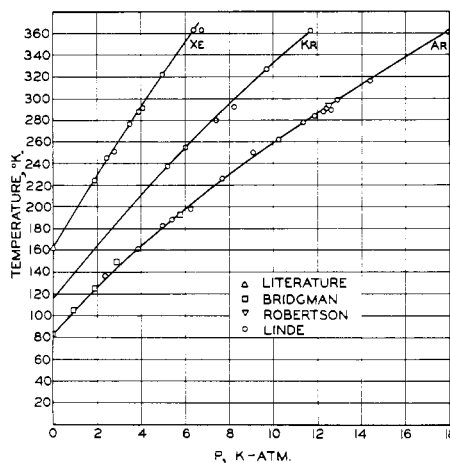


Figure 3. Melting temperature vs. pressure for argon, krypton, and xenon

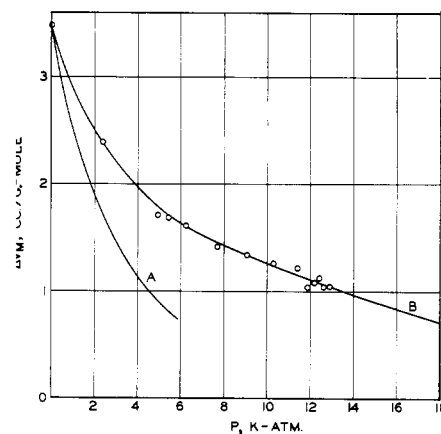


Figure 4. Volume change of argon during melting

Table I. Experimental Data on Fusion of Solid Argon

P , k-Atm.	T_m , ° K.	Fluid Vol., Cc./Gram-Mole	Solid Vol., Cc./Gram-Mole	ΔV of Fusion, Cc./Gram-Mole	Compressibility ($-dV/dP$), Cc./Gram-Mole Atm. $\times 10^3$	
					Fluid	Solid
2.389	137	27.07	24.67	2.4	1.398	0.963
4.972	182	25.49	23.78	1.71	1.025	0.566
5.417	188	25.55	23.85	1.70	1.104	0.533
6.249	197	24.89	23.27	1.62	0.786	0.393
7.690	226	24.23	22.82	1.41	0.744	0.393
9.100	245	23.77	22.43	1.34	0.546	0.341
10.250	262	23.55	22.28	1.27	0.494	0.393
11.366	278	23.30	22.09	1.21	0.380	0.285
11.898	284	23.08	22.03	1.05	0.482	0.277
12.236	288	22.86	21.77	1.09	0.401	0.356
12.440	291	23.05	21.93	1.12	0.339	0.318
12.670	290	22.76	21.72	1.04
12.960	299	22.46	21.42	1.04	0.391	...
14.413	317	22.32	0.338	...
18.040	360	20.99	20.30	0.69	0.337	...

values of P_0 and of c were determined by trial and error to fit the experimental data; the values thus obtained were 2234 atm. for P_0 and 1.5 for c .

The change in molar volume, ΔV_m , (cc. per gram mole) of argon during freezing or melting as a function of pressure is shown in Figure 4, together with a plot of Bridgman's data (2). The discrepancy between these two curves is discussed below.

A plot of P_m vs. T_m/V_m (Figure 5) was used to calculate the internal pressure, a , and the constant, γ , for the Grüneisen equation (4) relating the melting pressure of an inert gas to the ratio of temperature to molar volume of the solid:

$$P_m = 3\gamma RT_m/V_m - a$$

where R is the gas constant. A close fit of the high-pressure portion of the argon data, where the equation is valid, gives: $a = 5130$ atm., $3\gamma R = 1306$, and $\gamma = 5.305$.

Figure 6 shows the family of experimental isotherms plotted as molar volume vs. pressure in thousands of atmospheres. A smooth curve was first drawn through the experimental values of the molar volumes of argon gas at the onset of freezing. Then the volume changes during freezing from Figure 4 were measured vertically from this curve to locate the curve for the values of the molar volume of solid argon at the melting pressures. Compressibilities of gaseous and solid argon near the freezing point were smoothed graphically (Figure 7) and transferred to the appropriate locations along the freezing point envelope (Figure 6). Compressibilities of both gas and solid decrease with increasing pressure and approach the freezing zone asymptotically at high pressures (Figure 6). Although the volume change on freezing decreases with pressure, there is no indication that the fluid and solid volumes would ever be equal.

An equation for the solidus envelope of the above set of isotherms can be obtained by combining the Simon and Grüneisen equations:

$$V_m = (635.8) \frac{(P_m + 2234)^{2/3}}{P_m + 5130}$$

The broken line (Figure 6) is a graph of this combined

equation. Like the Grüneisen equation, it approaches the experimental curve closely at the higher pressures.

Thermodynamic values for the energy, ΔE_m , enthalpy, ΔH_m , and entropy, ΔS_m , of melting (or freezing) were computed from the Simon equation and the change in volume of argon during freezing as follows:

$$P_m/2234 = (T/83.2)^{1.5} - 1$$

$$dP_m/dT = 4.415 (T)^{1/2}$$

But

$$dP_m/dT = \Delta S_m/\Delta V_m$$

Therefore

$$\Delta S_m = 0.1069 \Delta V (T)^{1/2} \text{ cal./gram-mole-degree}$$

$$\Delta H_m = T\Delta S_m \text{ or } 0.1069 \Delta VT^{1.5} \text{ cal./gram-mole}$$

$$\Delta E_m = \Delta H_m - P_m\Delta V_m \text{ cal./gram-mole}$$

The computed values are listed in Table II. The energy of melting is relatively constant at 245 ± 5 cal. from 3000 to 12,000 atm. The enthalpy of melting increases until, at 12,000 atm., it reaches a maximum of 584 cal./gram-mole, which is more than double its value at atmospheric pressure. At higher pressures the enthalpy decreases.

RESULTS FOR KRYPTON

Krypton was compressed through its freezing pressure at temperatures ranging from 169° to 362° K. and pressures up to 12,000 atm. The experimental data are presented in Table III. At 293° K. the compressibilities of both gas and solid are approximately 0.7×10^{-3} cc./gram-mole atm.; the gas and solid compressibilities were not reliably determined for krypton.

Figure 3 shows the experimental values of melting temperature vs. pressure for krypton and the melting point at atmospheric pressure from the literature. A good fit for these points is obtained by the following form of the Simon equation:

$$P_m/3000 = (T_m/116.1)^{1.4} - 1$$

Figure 5 shows a graph of P_m vs. T_m/V_m for krypton.

Table II. Fusion of Solid Argon
(Derived thermodynamic data)

P , k -Atm	T , ° K.	V_g , Cc./Gram- Mole	V_s , Cc./Gram- Mole	ΔV , Cc./Gram- Mole	ΔS , Cal./Gram- Mole-Degree	ΔH , Cal./Gram- Mole	ΔE , Cal./Gram- Mole	$-dV_g/dP$, Cc./Gram- Mole-Atm., (Fluid)	$-dV_s/dP$, Cc./Gram- Mole-Atm., (Solid)
0	83.2°	28.1(3)	24.6(3)	3.5	3.4	282	282
1	107	27.4	24.5	2.9	3.3	344	273
2	127	26.8	24.3	2.5	3.0	387	265	...	1.13×10^{-3}
3	147	26.3	24.1	2.2	2.9	418	258	1.3×10^{-3}	0.85
4	165	25.8	23.9	1.9	2.7	444	254	1.15	0.86
6	199	25.0	23.4	1.6	2.4	484	249	0.86	0.49
8	230	24.3	22.9	1.4	2.3	528	253	0.65	0.38
10	259	23.6	22.4	1.3	2.2	564	256	0.50	0.31
12	286	23.0	21.8	1.1	2.1	584	256	0.41	0.28
14	312	22.3	21.3	1.0	1.9	578	246	0.36	...
16	337	21.6	20.8	0.8	1.6	550	228	0.34	...
18	378	21.0	20.3	0.7	1.4	528	236	0.32	...

Est.

Error $\pm 2\%$ $\pm 2\%$ $\pm 2\%$ $\pm 5\%$

° Melting temperatures up to 4 k -atm. from Bridgman's P - T data.

P = pressure, k -atm.
 T = temperature, ° K.
 V_g = volume of fluid, cc./gram-mole.
 V_s = volume of solid, cc./gram-mole.
 ΔV = expansion during fusion, cc./gram-mole.

ΔS = entropy of fusion, cal./gram-mole-degree.
 ΔH = enthalpy of fusion, cal./gram-mole.
 $-dV_g/dP$ = compressibility of fluid, cc./gram-mole-atm.
 $-dV_s/dP$ = compressibility of solid, cc./gram-mole-atm.

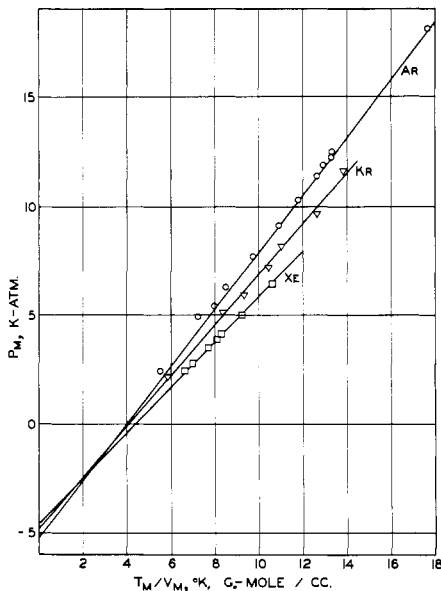


Figure 5. Melting pressure vs. ratio of melting temperature to molar volume for argon, krypton, and xenon

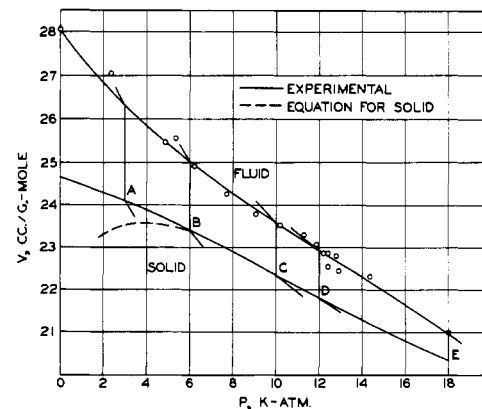


Figure 6. Compression isotherms of xenon near the freezing zone

- A. -127° C.
- B. -74° C.
- C. -14° C.
- D. 13° C.
- E. 86° C.

Figure 7. Compressibility of solid and gaseous argon near the freezing pressure

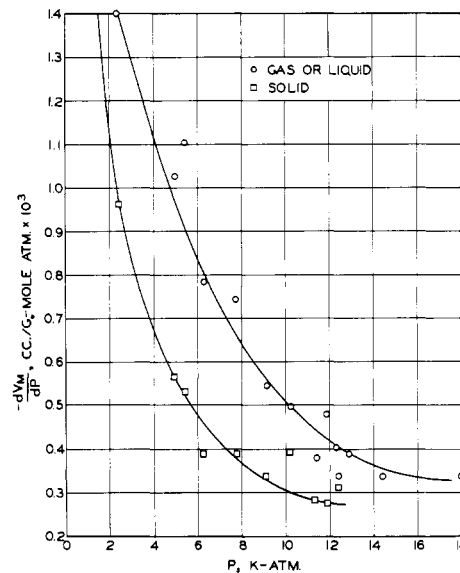


Table III. Experimental Data on Fusion of Solid Krypton

P , k-Atm.	T_m , ° K.	Fluid Vol., Cc./Gram- Mole	Solid Vol., Cc./Gram- Mole	ΔV of Fusion, Cc./Gram- Mole
0	116.1	34.13	29.65	...
2.16	169	32.0	28.9	3.08
5.12	237	30.5	28.4	2.11
5.96	255	29.4	27.4	1.99
7.21	280	28.5	26.8	1.77
8.19	293	28.2	26.7	1.50
9.65	327	27.6	26.0	1.55
11.62	362	27.3	26.3	1.02

The values for the constants γ and a in the Grüneisen equation were calculated from this curve. The equation becomes:

$$P_m = 1160 T_m / V_m - 4700$$

The value of γ is 4.71.

Several compression isotherms and the location of the freezing zone for krypton are shown in Figure 8, along with the low-temperature molar volumes of the liquid and solid as given in the literature (3). An approximate equation for the lower solidus envelope was obtained by combining the Simon and Grüneisen equations to eliminate T :

$$V_m = 443 \frac{(P_m + 3000)^{0.714}}{P_m + 4700}$$

The energy, enthalpy, and entropy of fusion of solid krypton, computed from the Simon equation and from the volume increase during fusion, are given in Table IV, together with a summary of smoothed PVT data.

RESULTS FOR XENON

Xenon was compressed to 22,000 atm. at several temperatures between 224° and 362° K. The experimental data are tabulated in Table V.

The Simon equation for xenon based on the graph of melting temperature vs. pressure (Figure 3) becomes:

$$P_m / 3400 = (T_m / 161.5)^{1.31} - 1$$

The Grüneisen equation for xenon, evaluated from the graph

(Figure 5) of the melting pressure vs. T_m / V_m , becomes:

$$P_m = 1042 T_m / V_m - 4570$$

where γ is 4.23.

Figure 9 is a graph of the compression isotherms for xenon showing the pressure-volume area of transition between solid and fluid xenon. The approximate solidus envelope curve as obtained by combining the Simon and Grüneisen equations is:

$$V_m = 340 \frac{(P_m + 3400)^{0.763}}{P_m + 4570}$$

Solid xenon was compressed well above the freezing pressure to obtain data on the compressibility up to 22,000 atm. The compressibility of xenon in cc./gram-mole atm., based on the slope of the isotherms at 15,000 atm., is 0.21×10^{-3} at 291° K. and 0.24×10^{-3} at 362° K. At a pressure of 22,000 atm., the compressibility is 0.15×10^{-3} over the temperature range of 279° to 362° K.

The energy, enthalpy, and entropy of fusion of solid xenon, computed from smoothed values of the ΔV of fusion and the Simon equation, are tabulated in Table VI along with other smoothed and derived values.

DISCUSSIONS

Qualitatively, the curves for xenon, krypton, and argon differ predictably. Xenon freezes at the lowest pressures. At equivalent pressures, xenon has the largest molar volume, and xenon also has the largest change in volume

during freezing and compression. The thermodynamic values for ΔE and ΔH of fusion are highest for xenon and lowest for argon, excepting the low values for krypton at 12,000 atm. Numerical constants in the Grüneisen and Simon equations for argon, krypton, and xenon show a logical progression with increase in atomic number.

ACCURACY OF EXPERIMENTAL DATA

Judging from the precision of the measurements and the scatter of the data from smoothed curves, the data are believed to be accurate to $\pm 2\%$ for the temperature, pressure, and volume, and to $\pm 5\%$ for the volume change

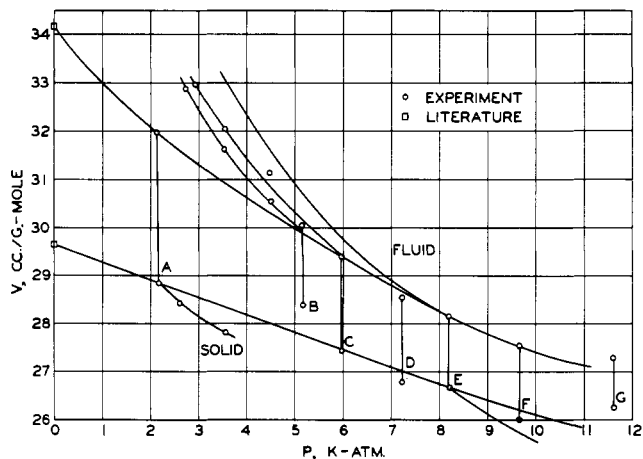


Figure 8. Compression isotherms of krypton near the freezing zone

- | | |
|----------------------------|--------------------------|
| A. -104°C. | D. 6°C. |
| B. -36°C. | E. 20°C. |
| C. -18°C. | F. 54°C. |
| D. -18°C. | G. 89°C. |

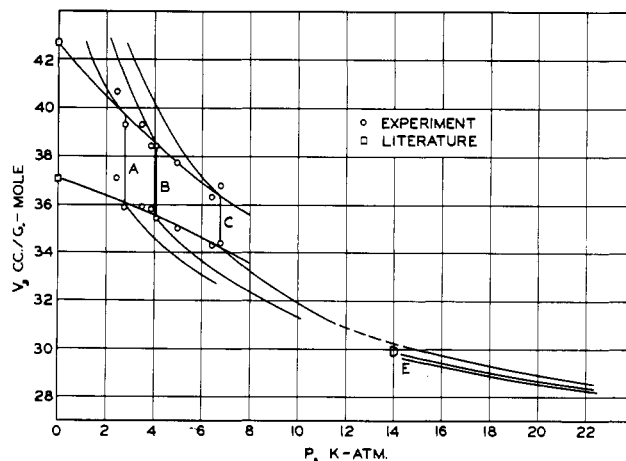


Figure 9. Compression isotherms of xenon near the freezing zone

- | | |
|---------------------------|--------------------------|
| A. -23°C. | D. 25°C. |
| B. 18°C. | E. 6°C. |
| C. 89°C. | |

Table IV. Fusion of Solid Krypton
(Derived data)

P , k-Atm.	T_m , $^{\circ}\text{K.}$	V_s , Cc./Gram- Mole	V_f , Cc./Gram- Mole	ΔV_m , Cc./Gram- Mole	ΔS_m , Cal./Gram- Mole-Degree	ΔH_m , Cal./Gram- Mole	ΔE_m , Cal./Gram- Mole
0	116.1	29.7(3)	34.1(3)	4.48	3.92	455	455
2	165	32.1	28.9	3.2	3.22	532	377
4	209	30.6	28.2	2.4	3.66	556	324
6	252	29.4	27.4	2.0	2.39	502	312
8	293	28.25	26.75	1.5	1.90	557	267
10	332	27.4	26.1	1.3	1.73	575	260
12	370	1.0	1.39	515	225

Table V. Experimental Data on Fusion of Solid Xenon

P , k-Atm.	T_m , $^{\circ}\text{K.}$	Fluid Vol., Cc./Gram-Mole	Solid Vol., Cc./Gram-Mole	ΔV of Fusion Cc./Gram-Mole	Compressibility (dV/dP), Cc./Gram-Mole-Atm. $\times 10^3$	
					Fluid	Solid
0	161.4	42.68	37.09	5.59
1.92	224	4.3
2.45	245	40.7	37.1	3.6
2.80	250	39.3	35.9	3.4	1.73	1.38
3.50	277	39.3	36.1	3.2
3.90	288	38.4	35.8	2.6
4.10	291	38.4	35.4	3.0	1.92	1.33
5.00	322.5	37.7	35.0	2.7
6.78	363	36.8	34.4	2.4	1.04	0.92
6.45	363	36.3	34.3	2.0

Table VI. Fusion of Solid Xenon
(Derived data)

P , k-Atm.	T_m , $^{\circ}\text{K.}$	V_s , Cc./Gram- Mole	V_f , Cc./Gram- Mole	ΔV_m , Cc./Gram- Mole	ΔS_m , Cal./Gram- Mole Degree	ΔH_m , Cal./Gram- Mole	ΔE_m , Cal./Gram- Mole
0	161.5	42.68(3)	37.09(3)	5.59	3.73	603	603
1	198	41.5	36.8	4.7	3.34	662	548
2	231	40.5	36.5	4.0	2.99	690	495
3	262	39.5	36.1	3.4	2.64	691	444
4	292	38.6	35.6	3.0	2.41	704	413
5	322	37.6	35.1	2.5	2.07	665	364
6	351	26.9	34.7	2.2	1.87	655	336
7	379	36.2	34.2	2.0	1.74	662	323
8	406	35.6	33.7	1.9	1.69	685	317

on freezing. The gases are presumed to be sufficiently pure to exclude significant systematic errors due to contaminants.

The large difference between the volume change of argon during freezing found in these experiments and the volume change reported by Bridgman (2) (Figure 4) cannot be ignored. There are differences ranging from 35 to 100% between Bridgman's results and those of the authors. Any possible error in the piston-displacement method used in the present work would not seem large enough to account for this discrepancy. "Squaring-up" the experimental curve of displacement *vs.* pressure could lead to slightly too high a value, although no difficulty was found in reproducing the published data on the change in volume of water during freezing at comparable pressures. An undiscovered leak of gas prior to measuring the argon sample volume after the experiment, and an equivalent error in computing the sample size at the start of the experiment (from the vessel size and published *PVT* data on argon) would be an unlikely coincidence.

Bridgman pointed out that his bulb-filling method could be in error on the low side if the filling capillary became

plugged with solid. This might possibly explain why Bridgman reported lower values than these.

ACKNOWLEDGMENT

The authors acknowledge the assistance of H.L. Williams, who performed most of the experimental work. They are also grateful to G.A. Cook for valuable editorial assistance.

LITERATURE CITED

- (1) Birch, F., Robertson, E.C., Office of Naval Research, Tech. Rept. NR-32400 (1957).
- (2) Bridgman, P.W., *Proc. Am. Acad. Arts Sci.* **70**, 1 (1935).
- (3) Clusius, K., Weigand, K., *Z. phys. Chem.* **B46**, 1 (1940).
- (4) Grüneisen, E., "Handbuch der Physik," Vol. 10, p. 22, Springer, Berlin, 1926.
- (5) Robinson, D.W., *Proc. Roy. Soc.* **A225**, 393 (1954).
- (6) Simmon, F.E., Ruhemann, M., Edwards, W.A.M., *Z. phys. Chem.* **B6**, 62, 331 (1930).

RECEIVED for review March 13, 1961. Accepted July 14, 1961.

Velocity of Sound in Compressed Gases

T. K. SHERWOOD

Massachusetts Institute of Technology, Cambridge, Mass.

VALUES of the velocity of sound in compressed gases are required for various technical purposes, as for the design of pulsation dampeners and the calculation of throat velocities in supersonic nozzles. Few data are available and the sound velocity must usually be calculated from other properties of the gas. Simple formulas are available for ideal gases, which serve adequately for many purposes, but these are not useful if the gas properties differ appreciably from ideality.

Reliable values of the sound velocity may be obtained if the low-pressure heat capacity and an accurate equation of state for the gas in question are known. The present study explores the possibility that useful values of sound velocity might be calculated from a general reduced equation of state for all gases. The results are compared with limited experimental data on CH₄, C₂H₄, C₂H₆, C₃H₈, i-C₅H₁₂, n-C₅H₁₂, He, and CO₂.

Thermodynamics provides the following relations:

$$C^2 = -av^2 \left(\frac{\partial P}{\partial v} \right)_s = \frac{a RT K Z^2}{Z - P_r \left(\frac{\partial Z}{\partial P_r} \right)_{T_r}} \quad (1)$$

$$K = \frac{C_p}{C_v} = \frac{C_p^0 + \Delta C_p}{(C_p^0 + \Delta C_p) - (C_p - C_v)} \quad (2)$$

$$\Delta C_p = \frac{\partial}{\partial T_r} \left(\frac{H - H^0}{T_c} \right)_{P_r} \quad (3)$$

$$C_p - C_v = \frac{R \left[Z + T_r \left(\frac{\partial Z}{\partial T_r} \right)_{P_r} \right]^2}{Z - P_r \left(\frac{\partial Z}{\partial P_r} \right)_{T_r}} \quad (4)$$

Here *C* is the sound velocity and *Z* is the compressibility

For estimating sound velocities, the tables in this article give greater accuracy than graphs. The tables are also practical for other purposes—for example, data on heat capacity function have been published by Edmister and by Lyderson, Greenkorn, and Hougen, based on earlier generalized equations of state. The present data, based on Pitzer's recent work, are calculated by numerical differentiation.

factor, which is assumed to vary only with *P_r* and *T_r*, the reduced pressure and the reduced temperature, respectively. The above relations are the same as those used by Buthod and Tien (1) in a recent similar study.

Of the several reduced equations of state available, that of Pitzer and Curl (12) was selected, values of *Z* being taken from their tables for *Z_c* = 0.27 (this is equivalent to an "acentric factor," ω, of 0.2625, since *Z_c* = 0.291 - 0.08 ω). Values of ∂*Z*/∂*P_r* and ∂*Z*/∂*T_r* were obtained from large graphs of *Z vs. P_r* or *T_r*, using numerical or graphical methods, as seemed appropriate. Values of Δ*C_p* were obtained in the same manner, using Pitzer and Curl's values of (H - H⁰)/*T_c*.

The result of these calculations is three functions:

$$C^2/aRTK = f_1(P_r, T_r) \quad (\text{Table I})$$

$$\Delta C_p = f_2(P_r, T_r) \quad (\text{Table II})$$

$$C_p - C_v = f_3(P_r, T_r) \quad (\text{Table III})$$

Values of *C_p⁰* needed in Equation 2 are available from API Research Project 44 (2, 14).

Using these tables, values of *C* are calculated as follows: *P_r* and *T_r* are obtained as ratios of the specified temperature and pressure to the known critical properties [if *P_c* and *T_c* are not known, they may be estimated closely by the methods described by Reid and Sherwood (13)]; Δ*C_p* and *C_p* - *C_v* are found from Tables II and III and *K* is calculated from *C_p⁰* using Equation 2; *C²/aRTK* is obtained from Table I, and *C* calculated by substitution.

The procedure will be illustrated by estimating *C* for ethane at 90° F. and 116 atm. From the literature, *P_c* = 48.3 atm., *T_c* = 550° R., and *C_p⁰* = 12.8; whence *P_r* = 2.4 and *T_r* = 1.00. From Tables II and III Δ*C_p* = 16.53, *C_p* - *C_v* = 15.93,